Improvement of the performance of a grid connected photovoltaic system by direct power control strategy with a new switching table

Amrani Mohamed Nader **Dib Abederrahmane**
University Oum El Bouaghi
Amranimednader@yahoo.fr, dibabderrahmane@yahoo.fr
Annane Mohamed Mustapha
University ferhat abbas, sétif
annanemustapha@yahoo.fr

Abstract: *Solar energy is the most powerful permanent, clean and renewable energy source that has the potential of changing the future of the world. The use of solar energy, principally photovoltaic, for different applications mainly electrical grid, is well suited for most rural areas due to the lack of electrification, but also for a large number of the countries around the world. Here, we propose a strategy for optimizing the performance of a grid-connected photovoltaic power system. To achieve this, we used the maximum power point tracking (MPPT) control method based on the fuzzy logic controlled. To control and improve the performances of a voltage source inverter for grid connected photovoltaic systems, we used the newly developed direct power control technique. We created simulations of the proposed approach MATLAB / Simulink and found very interesting results compared to the existing control strategies in this field.*

Key words: *Grid-connected photovoltaic system, MPPT, direct power control, new switching table.*

I. INTRODUCTION

Solar energy is one of the most powerful and promising alternative energies that can be an alternative to fossil energy [1]. The United Nations Development Programme in its 2000 World Energy Assessment estimated the potential of solar energy at 1,575-49,387 Exajoules (EJ). This potential is significantly higher than the world energy consumption altogether, which was estimated at 559.8 EJ in 2012. Solar energy is recommended as a sustainable source for its increasing economic benefits over the diminishing reserves of fossil fuel as well as for reasons related to environment protection. Photovoltaic (PV) system based on a special technology for converting the solar rays to electrical power is one of the main applications of solar energy [1]. PV systems are commonly easy to install with low maintenance operation requirements [2]. There are two types of PV systems namely, autonomous system and grid connected system. The most important field of PV application is the grid connected photovoltaic system.

PV systems connected to the grid are structured with a solar generator, two static converters and an electrical grid. The first converter is a DC-DC converter controlled by a maximum power point tracking (MPPT) to get a maximum power point of photovoltaic generator (PVG). The second converter is a three-phase inverter used to convert the DC into AC injected into the electrical grid.

The MPPT controller plays a critical role in the PV power system for maximizing the PVG power. The control principle is based on the automatic variation of the duty cycle to the appropriate value. There are different algorithms types for the MPPT controller [3]. Due to its simplicity, the Perturb and Observe algorithm (P&O) is the most commonly used to search the maximum power point. It requires only voltage and current measurements of the PVG. The operating principle of the P&O algorithm is based on voltage perturbation of voltage and observing observation of the impact of this change on the output power of the PV panel. However, this method has a major disadvantage represented by the problem of oscillations around the MPPs.

Recently, new artificial intelligence methods were developed for avoid disadvantage of classical MPPT [4-5]. These methods identify the maximum power point tracking (MPPT) algorithm based on the artificial neural networks (ANN) technique. Fuzzy logic controller has been demonstrated to obtain the optimum power point with good performance compared with other algorithm [6].

To convert the DC into AC, the three-phase voltage source inverter is the most topology used regarding to its simplicity and robustness. There are two principal methods to control the inverter, the direct and the indirect. The objective of these methods is to improve the current signal shape and reduce harmonic distortion.
The pulse wide modulation (PWM) method is the most commonly used to control the voltage source inverter due to its simplicity. The PWM has some disadvantages, such as unwanted harmonic and a poor transient response. The best

method used in direct control of grid-connected is direct power control (DPC). This strategy is inspired the principle of direct torque control (DTC) of AC machines [7]. The converter switching states are selected by a switching table .The voltage vector position and the outputs of hysteresis correctors represent the inputs of switching table [8]. In this study, we proposed a novel switching table for direct power control of three-phase voltage source inverter. We also describe the topology for the PV array and boost converter with the MPPT control, and a direct power control with new switching table. Our simulation results show the variations of current, voltage and total harmonic distortion. The results analysis confirms that the proposed model given the good performances with a much reduced total harmonic distortion (THD). The current and voltage profiles have a sinusoidal form with a very little with a power factor unity.

In this paper, the first section describes the mathematical models of the PV array and boost converter. The used MPPT control is presented in the second section. In the third section, the direct power controller principle is demonstrated with the syntheses the new switching table. The proposed system is presented in the fifth section. Finally in the sixth section, we present a simulation and discussion of the results obtained in this study.

II. MATHEMATICAL MODEL OF THE SOLAR PANEL:

There are several mathematical models representing the operation of a photovoltaic generator. In this study, we used the electric model represented by the following figure [9].

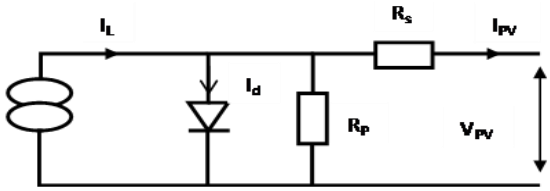

Fig.1. The solar cell.

The output current of the solar cell is given by

$I_{pv} = I_L - I_d - I_p$

Where: $I_L = N_p . I_{pv}$

By considering the electrical characteristics of a junction, this current can be given by [3]

$$I_{pv} = I_L - I_o\left(e^{\frac{q\left(V_{pv}+I_{pv}R_s\right)}{V_T}} - 1\right) - \frac{V_{pv}+I_{pv}R_s}{R_p} \quad (1)$$

The ideal photovoltaic module is the one for which R_s is zero and R_p is infinitely great. The output current and voltage are then given by

$$I_{pv} = I_L + I_o\left(e^{\frac{\left(V_{pv}\right)}{V_T}} - 1\right) \quad (2)$$

$$V_{pv} = V_T \ln\left(\frac{I_L - I_{pv}}{I_o} + 1\right) \quad (3)$$

Where:

N_s: number of cells connected in series, N_p: number of cells connected in parallel, R_s: series resistance, R_p: parallel resistance, I_{sc} : short circuit current, I_d: current of the diode, I_{pv}: output current and of the solar cell, I_L : current generated by the solar modules, I_o: saturation current of the diode , V_{pv}: output voltage of the solar cell

III. BOOST CONVERTER

The boost converter is principally composed by Electronics components. It is used in several domains. In this case, the boost converter coupled with PVG. To maintain the power of PVG near to the maximum power point whatever the illumination variations are, the MPPT controller that generates the duty cycle will be controlled by the MOSFET of Boost converter. The following figure shows circuit the boost converter:

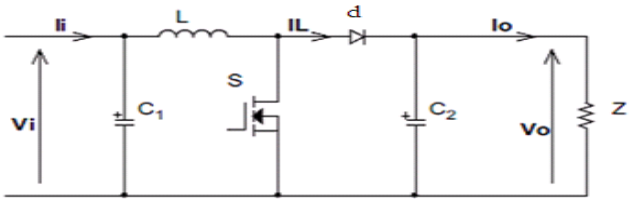

Fig.2 the Boost converter.

The mathematical model of the DC-DC converter expressed by the following equations: [10], [11]

$$\frac{V_o}{V_i} = \frac{1}{1-D} \quad (4)$$

$$\frac{I_i}{I_o} = \frac{1}{1-D} \quad (5)$$

Where:

I_i: input current, I_o: output current, V_i: input voltage, V_o: output voltage, D: duty cycle

IV. MPPT CONTROLLER OF PV SYSTEMS USING FUZZY LOGIC CONTROLLER (FLC)

In general, a fuzzy logic controller is divided into the following three blocks [6]: 1) the fuzzification to convert real variables to fuzzy variables, 2) the inference where these variables are compared with predefined sets to determine appropriate response, 3) the defuzzification to convert the subset fuzzification into values [12].

The basic structure of our fuzzy controller is shown in Figure [12].

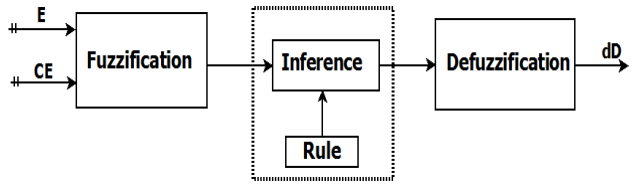

Fig.3. Basic structure of fuzzy controller.

In the following section, we will detail the steps achievements of fuzzy logic controller, which comprises the next three blocks:

1. Fuzzification

The membership functions assigned to the linguistic variables, using five fuzzy sets. The triangular and trapezoidal functions are used.

The used system consists of two input variables, error (E) and the change of the error (ΔE) expressed as follows:

$$E(k) = \frac{P(k) - P(k-1)}{V(k) - V(k-1)} \quad (6)$$

$$\Delta E(k) = E(k) - E(k-1) \quad (7)$$

The universe of discourse of the input variable E and ΔE is allocated based on linguistic variable with five fuzzy sets which are designated by very negative (VN), negative (NS), zero (ZE), positive (PS) and very positive (VP).

2. Fuzzy inference:

In the literature, several methods are proposed composition such as Max-Min and Max-Dot. In this study, we opted for the use of the Mamdani fuzzy inference method.

CE / E	VN	NS	ZE	PS	VP
VN	ZE	ZE	PM	VP	VP
NS	ZE	ZE	PS	PS	PS
ZE	PS	ZE	ZE	ZE	NS
PS	NS	NS	NS	ZE	ZE
VP	VN	VN	VN	ZE	ZE

TABLE 1 TABLE OF FUZZY RULES.

3. Defuzzification

The output variable is the duty cycle. Defuzzification uses the center of gravity.

$$dD = \frac{\sum_{j=1}^{n} \mu(D_j) - D_j}{\sum_{j=1}^{n} \mu(D_j)} \quad (8)$$

The output variable dD is allocated based a linguistic variable with five fuzzy sets which are designated by very negative (VN), negative (NS), zero (ZE), positive (PS), and positive (VP).

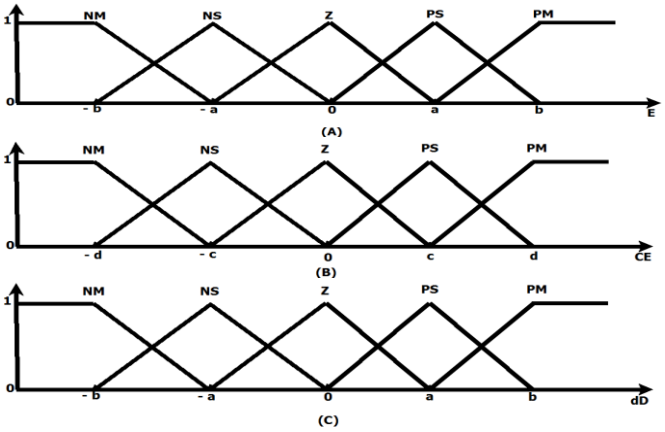

Fig.4. Definitions and membership functions of (a) the 1st input variable (E), (b) the 2nd input variable (CE) and (c) the output variable (dD).

V. DIRECT POWER CONTROL

Figure (5) presented the diagram of direct power control. Two types of sensors are required for measured the voltage and the current line of the electrical grid. The value of voltage and current allow estimation of the reactive and active powers by equation (9).

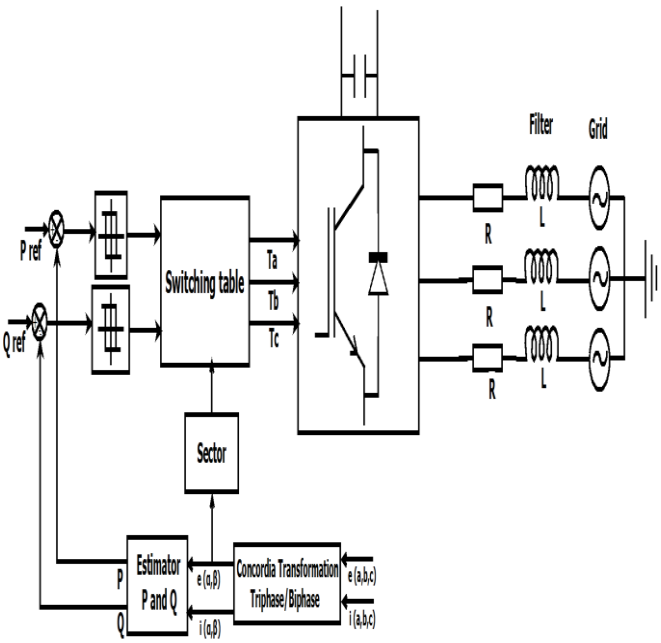

Fig.5. The diagram of direct power.

$$P = i_\alpha . e_\alpha + i_\beta . e_\beta$$
$$q = i_\alpha . e_\beta - i_\beta . e_\alpha \quad (9)$$

Using of concordia transformation, the voltage and the current vector are given by the following equations

$$e_{\alpha\beta} = \begin{bmatrix} e_\alpha \\ e_\beta \end{bmatrix} = \sqrt{\frac{2}{3}} \begin{bmatrix} 1 & -1/2 & -1/2 \\ 0 & \sqrt{3}/2 & -\sqrt{3}/2 \end{bmatrix} \begin{bmatrix} e_a \\ e_b \\ e_c \end{bmatrix} \quad (10)$$

Also we can write it in another way;

$$e_\alpha = E.\cos(\theta) \quad \text{and} \left\| e_{\alpha\beta} \right\| = E \quad (11)$$
$$e_\beta = E.\sin(\theta)$$

$$i_{\alpha\beta} = \begin{bmatrix} i_\alpha \\ i_\beta \end{bmatrix} = \sqrt{\frac{2}{3}} \begin{bmatrix} 1 & -1/2 & -1/2 \\ 0 & \sqrt{3}/2 & -\sqrt{3}/2 \end{bmatrix} \begin{bmatrix} i_a \\ i_b \\ i_c \end{bmatrix} \quad (12)$$

The reference value of active and reactive power are given directly as constant and compared with the value estimate of P and q. The results of this comparison presented input of the hysteresis comparators; the output of the hysteresis comparators is digitized variable S_p and S_q follows:

$$S_p = 1 \quad \text{if} \quad P^* - \hat{P} \geq h_p \qquad S_p = 0 \quad \text{if} \quad P^* - \hat{P} \leq -h_p$$
$$S_q = 1 \quad \text{if} \quad q^* - \hat{q} \geq h_p \qquad S_q = 0 \quad \text{if} \quad q^* - \hat{q} \leq -h_p$$

The line voltage vectors position determined by equation (13)

$$\theta_n = \text{arctg}\left(V_{s\alpha} / V_{s\beta} \right) \quad (13)$$

The switching table has three inputs are: 1) the digitized variable S_p, S_q and θ_n, 2) the output is the switching state S_a, S_b and S_c of the inverter, 3) the conventional switching table is presented in table 2

S_p	S_q	θ_1	θ_2	θ_3	θ_4	θ_5	θ_6	θ_7	θ_8	θ_9	θ_{10}	θ_{11}	θ_{12}
1	0	V_6	V_7	V_1	V_0	V_2	V_7	V_3	V_0	V_4	V_7	V_5	V_0
	1	V_7	V_7	V_0	V_0	V_7	V_7	V_0	V_0	V_7	V_7	V_0	V_0
0	0	V_6	V_1	V_1	V_2	V_2	V_3	V_3	V_4	V_4	V_5	V_5	V_6
	1	V_1	V_2	V_2	V_3	V_3	V_4	V_4	V_5	V_5	V_6	V_6	V_1

TABLE 2 SWITCHING TABLE OF CLASSICAL DIRECT POWER CONTROL

With $V_1(100)$,$V_2(110)$, $V_3(010)$, $V_4(011)$, $V_5(001)$, $V_6(101)$, $V_0(000)$, $V_7(111)$.

In this paper, we developed a new switching table to overcome the challenges and disadvantages of using a classic DPC.

1. Synthesis of the switching table

For the balanced three phase's system, in the reference α-β the current is expressed by the following relationship;

$$\frac{di_\alpha}{dt} = \frac{1}{L}(e_\alpha - v_\alpha - R.i_\alpha)$$
$$\frac{di_\beta}{dt} = \frac{1}{L}(e_\beta - v_\beta - R.i_\beta) \quad (14)$$

From equation (14) we can notice that the current $[i_\alpha\ i_\beta]^t$ depends on several factors; voltage vector of the electrical grid, Vector control and actual current.

Practically, the parameter R effect is neglected.

$$\frac{di_\alpha}{dt} = \frac{1}{L}(e_\alpha - v_\alpha)$$
$$\frac{di_\beta}{dt} = \frac{1}{L}(e_\beta - v_\beta) \quad (15)$$

The derivation of the equation (9) obtained:

$$\frac{dP}{dt} = i_\alpha \frac{de_\alpha}{dt} + e_\alpha \frac{di_\alpha}{dt} + i_\beta \frac{de_\beta}{dt} + e_\beta \frac{di_\beta}{dt}$$
$$\frac{dq}{dt} = i_\alpha \frac{de_\beta}{dt} + e_\beta \frac{di_\alpha}{dt} - i_\beta \frac{de_\alpha}{dt} - e_\alpha \frac{di_\beta}{dt} \quad (16)$$

The period of the grid voltage is very large compared to the switching period, we can write

$$e_{\alpha\beta}(k) = e_{\alpha\beta}(k+1)$$

$$\frac{dP}{dt} = e_\alpha \frac{di_\alpha}{dt} + e_\beta \frac{di_\beta}{dt}$$
$$\frac{dq}{dt} = e_\beta \frac{di_\alpha}{dt} - e_\alpha \frac{di_\beta}{dt} \quad (17)$$

By the discretization of the first order, the equation of (current, power) on a switching period Ts becomes the form;

$$\Delta i_\alpha = i_\alpha(k+1) - i_\alpha(k) = \frac{T_s}{L}(e_\alpha(k) - v_\alpha(k)) \quad (18)$$
$$\Delta i_\beta = i_\beta(k+1) - i_\beta(k) = \frac{T_s}{L}(e_\beta(k) - v_\beta(k))$$

$$\begin{cases} \Delta P = e_\alpha(k).\Delta i_\alpha + e_\beta(k).\Delta i_\beta \\ \Delta q = e_\beta(k).\Delta i_\alpha - e_\alpha(k).\Delta i_\beta \end{cases} \quad (19)$$

By substituting the equation (18) in (19), we obtain

$$\Delta P = \frac{T_s}{L}\left(e_\alpha^2(k) + e_\beta^2(k) \right) - \frac{T_s}{L}\left(e_\alpha(k).v_\alpha(k) + e_\beta(k).v_\beta(k) \right)$$
$$\Delta q = \frac{T_s}{L}\left(e_\alpha(k).v_\beta(k) - e_\beta(k).v_\alpha(k) \right) \quad (20)$$

By observation of equation (20) it can be concluded that the change of active and reactive power depends on the voltage vector from the electrical grid and the control vector.

The following expression delineates the instantaneous change of active and reactive power:

$$\Delta P_i = \frac{T_s}{L}\left(e_\alpha^2(k)+e_\beta^2(k)\right)-\frac{T_s}{L}\left(e_\alpha(k).v_{\alpha i}+e_\beta(k).v_{\beta i}\right)$$

$$\Delta q_i = \frac{T_s}{L}\left(e_\alpha(k).v_{\beta i}-e_\beta(k).v_{\alpha i}\right)$$

$$i=0.....6. \qquad (21)$$

The; $$e_\alpha^2(k)+e_\beta^2(k)=\frac{3}{2}E_m^2 \qquad (22)$$

It is assumed that $E^2=\frac{3}{2}E_m^2$

By Substituting equations (11) and (22) into (21) we obtain

$$\begin{cases}\Delta P_i = \frac{T_s}{L}\|E\|^2-\frac{T_s}{L}\|E\|.\left[\cos(\theta).v_{\alpha i}+\sin(\theta).v_{\beta i}\right]\\ \Delta q_i = \frac{T_s}{L}\|E\|.\left[\cos(\theta).v_{\beta i}-\sin(\theta).v_{\beta i}\right]\end{cases} \qquad (23)$$

Figures (6) and (7) are the standard variation of the active and reactive power in all sectors.

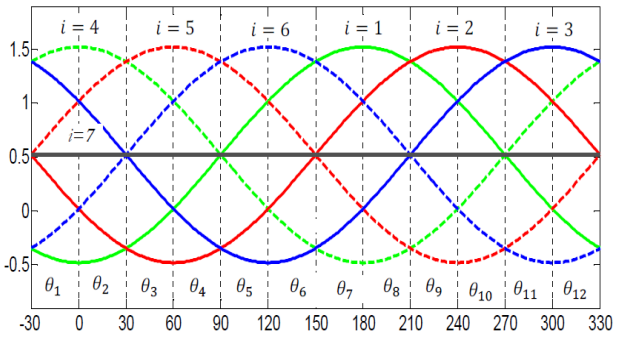

Fig. 6. Change in instantaneous active power.

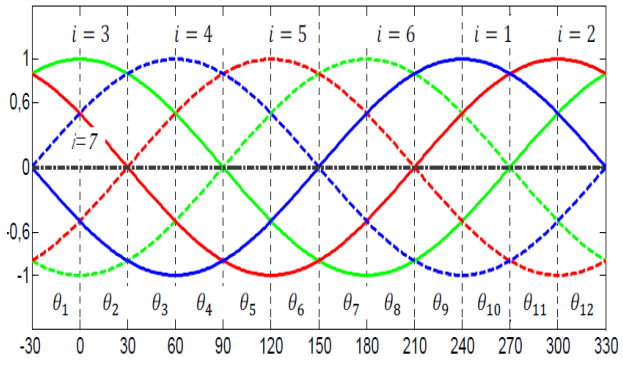

Fig. 7. Change in instantaneous reactive power.

For each sector, the knowledge of the sign and the change of active and reactive power for each sector are required to synthesize switching table. As an example, Tables 3 and 5 show change of active and reactive power in sectors 1 and 2, respectively. Tables 4 and 6 show the control vector for each combination of Sp and Sq in sectors 1 and 2, respectively

$\dot{\bar{P}}_1>0$	$\dot{\bar{P}}_1<0$	$\dot{\bar{q}}_1>0$	$\dot{\bar{q}}_1<0$	$\dot{\bar{P}}_1=0$
V_3, V_4, V_5, V_0	V_1, V_6	V_1, V_2, V_3	V_4, V_5, V_6	V_0, V_7

TABLE 3 SUMMARIZES ALL THE CHANGES OF ACTIVE AND REACTIVE POWER IN SECTOR 1

Sector 1	$\dot{\bar{q}}>0 \Leftrightarrow S_q=1$	$\dot{\bar{q}}<0 \Leftrightarrow S_q=0$
$\dot{\bar{P}}>0 \Leftrightarrow S_P=1$	V_3	V_4, V_5
$\dot{\bar{P}}<0 \Leftrightarrow S_P=0$	V_1	V_6

TABLE 4 SHOWS THE CONTROL VECTORS SELECTED IN SECTOR 1, FOR EACH COMBINATION OF S_P AND S_q

$\dot{\bar{P}}_2>0$	$\dot{\bar{P}}_2<0$	$\dot{\bar{q}}_2>0$	$\dot{\bar{q}}_2<0$	$\dot{\bar{P}}_2=0$
V_3, V_4, V_5, V_0	V_1, V_2	V_2, V_3, V_4	V_1, V_5, V_6	V_0, V_7

TABLE 5 SUMMARIZES ALL THE CHANGES OF ACTIVE AND REACTIVE POWER IN SECTOR 2

Sector 2	$\dot{\bar{q}}>0 \Leftrightarrow S_q=1$	$\dot{\bar{q}}<0 \Leftrightarrow S_q=0$
$\dot{\bar{P}}>0 \Leftrightarrow S_P=1$	V_3, V_4	V_5
$\dot{\bar{P}}<0 \Leftrightarrow S_P=0$	V_2	V_1

TABLE 6 SHOWS THE CONTROL VECTORS SELECTED IN SECTOR 2, FOR EACH COMBINATION OF S_P AND S_Q

The proposed switching table is:

S_p	S_q	θ_1	θ_2	θ_3	θ_4	θ_5	θ_6	θ_7	θ_8	θ_9	θ_{10}	θ_{11}	θ_{12}
1	0	V_5	V_6	V_6	V_1	V_1	V_2	V_2	V_3	V_3	V_4	V_4	V_5
	1	V_2	V_3	V_3	V_4	V_4	V_5	V_5	V_6	V_6	V_1	V_1	V_2
0	0	V_6	V_1	V_1	V_2	V_2	V_3	V_3	V_4	V_4	V_5	V_5	V_6
	1	V_1	V_2	V_2	V_3	V_3	V_4	V_4	V_5	V_5	V_6	V_6	V_1

TABLE 7 THE PROPOSED SWITCHING TABLE

VI. DESCRIPTION OF THE CONTROL SYSTEM

The grid-connected photovoltaic power system proposed in this work consists of a solar generator, two static converters and a electrical grid. The following figure shows our proposed system:

Among the two converters: the one is called chopper and is controlled by a MPPT to obtain the maximum power point; and the second converter is called three-phase inverter, and converts the DC into AC.

For this, we proposed a system that is mainly composed of two parts of command:

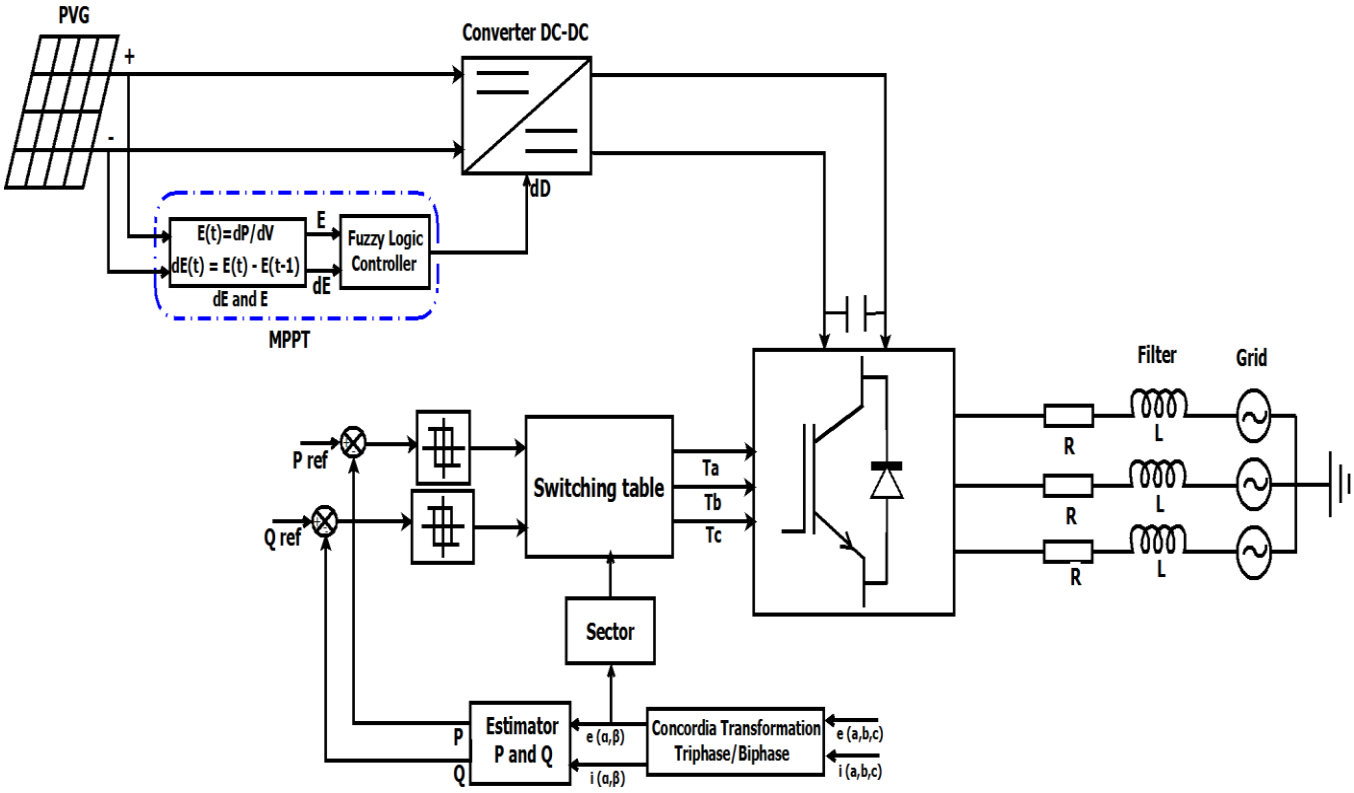

Fig.8 Block diagram of a grid-connected PV system.

1 - MPPT Controller based on the FLC to obtain a control signal of the appropriate variable step and improve the performance of photovoltaic generator.

2 – DPC control to enhance the performance of the electrical grid.

VII. SIMULATION RESULTS

The simulation results of the proposed system were generated using Matlab / Simulink. In this case, we used the following values as standard conditions: 25 °C for temperature and an solar radiation of 1000W/m^2.

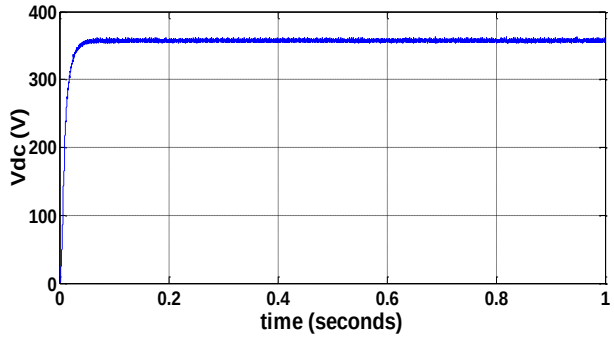

Fig.9. DC Bus Voltage.

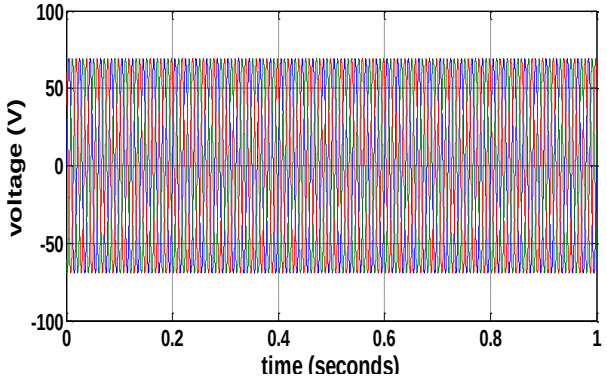

Fig.10. Phase a voltage.

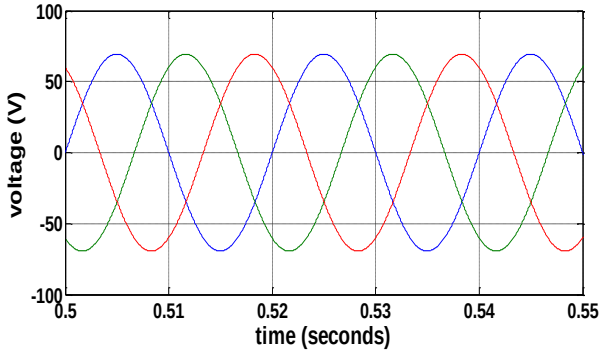

Fig.11. Zoom of phase a voltage.

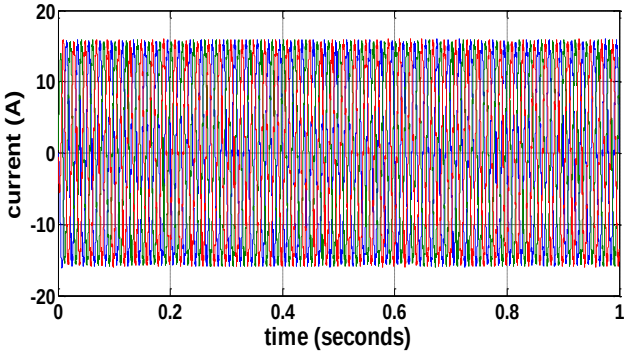

Fig.12. Phase a current.

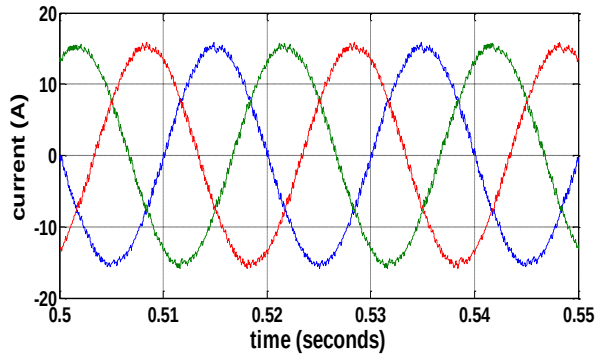

Fig.13. Zoom of phase a current.

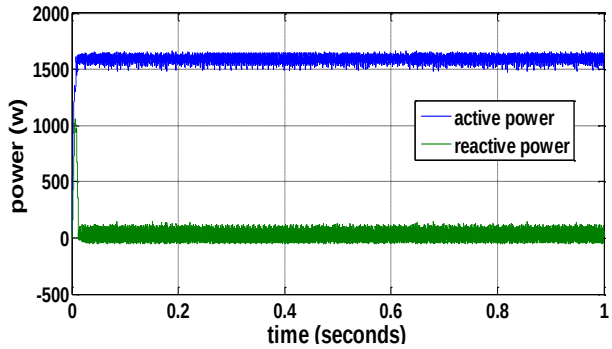

Fig.14. Active and reactive grid power.

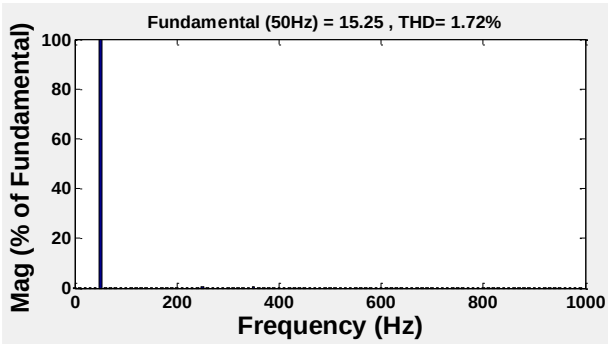

Fig.15. Total harmonic distortion.

In this section, we discuss the performance of the proposed system. Figure 9 represents the voltage of DC Bus. Figure 12 shows the response of the phase to the current and graph 10 represents the response of the phase to a voltage. Responses of the active and the reactive are shown in figure 14 for constant operating conditions.

The search for maximum power point based on FLC control shows that: "The optimal point is achieved for an optimal PVG voltage with a short transitory regime.

By carefully observing the obtained results, we feel confident that the proposed conversion chain has a good performance with low harmonic distortion for the line currents (around 1.72 %), which confirms that line current has been acceptable.

VIII. CONCLUSION

Our study presented here applies generally for the optimization of a grid-connected photovoltaic power system performance. To achieve this, we have used the control modern techniques based on fuzzy logic control and direct power control. A simulation result shows that, the proposed system improves the performance of the grid-connected photovoltaic power system. The MPPT control gives a quick response, reduced power oscillations around the optimal point and is more effective than the conventional control devices developed so far. The Inverter is controlled by direct power control. This method actually gives a good response. Finally, simulation results show a very good performance of the proposed system.

REFERENCES

[1] Hyun-Su Bae, Joung-Hu Park, Bo-Hyung Cho, Gwon-Jong Yu, New MPPT Control Strategy for Two-Stage Grid-Connected Photovoltaic Power Conditioning System, Journal of Power Electronics, Vol. 7, No. 2, April 2007.

[2] Esram T., Kimball J.W., Krein P.T., Chapman P.L., Midya P., "Dynamic maximum power point tracking of photovoltaic arrays using ripple correlation control, " IEEE Trans Power Electron, vol. 21, pp. 1282–1291, 2006.

[3] Mohamed A. AWADALLAH, Fawzan SALEM "Neuro-Fuzzy modeling and MPPT control of photovoltaic arrays feeding VSI induction motor drives" journal of electrical engineering.

[4] Bouzelata Yahia, Djeghloud Hind, Chenni Rachid, "The Application of an Active Power Filter on a Photovoltaic Power Generation System", International journal of renewable energy research, Vol.2, 2012.

[5] Hanen Abbes, Hafedh Abid, Kais Loukil, "An Improved MPPT Incremental Conductance Algorithm Using T-S Fuzzy System for Photovoltaic Panel", International journal of renewable energy research, Vol.5, 2015.

[6] Ahmed G. Abo- Khalil, Dong- Choon Lee, Jong-Woo Choi, Heung-Geun Kim, Maximum Power Point Tracking Controller Connecting PV System to Grid, Journal of Power Electronics, Vol. 6, No. 3, July 2006.

[7] Sergio Aurtenechea, Miguel Angel Rodríguez, Estanis Oyarbide, José Ramón Torrealday, Predictive Direct Power Control - A New Control Strategy for DC/AC Converters, (2010).

[8] Abdelouahab Bouafia, Jean-Paul Gaubert; and Fateh Krim, "Analysis and Design of New Switchin Table for Direct Power Control of Three-Phase PWM Rectifier", 2008.

[9] Azzouzi. M. Optimization of Photovoltaic Generator by Using P&O Algorithm under Different, 2013.

[10] Ritesh Keshri a , Manuele Bertoluzzo a & Giuseppe Buja, "Integration of a Photovoltaic Panel with an Electric City Car", Electric Power Components and Systems, vol. 42, pp. 481–495, 2014.

[11] M. Nabil a , S. M. Allam b & E. M. Rashad, "Performance Improvement of a Photovoltaic Pumping System Using a Synchronous Reluctance Motor", Electric Power Components and Systems, vol.41, pp.447–464, 2013.

[12] Josephine. R. L, dhayal raj, padmabeaula, helen catherine R. L "simulation of incremental conductance MPPT with direct Control and fuzzy logic methods using Sepic converter" journal of electrical engineering.